Time Release of Encapsulated Additives for Enhanced Performance of Lithium-Ion Batteries

Tae-Wook Lim,[†,§] Chan Woo Park,[§,∥] Scott R. White,[‡,§] and Nancy R. Sottos*[,†,§]

[†]Department of Materials Science and Engineering, [‡]Department of Aerospace Engineering, and [§]Beckman Institute for Advanced Science and Technology, University of Illinois at Urbana-Champaign, Urbana, Illinois 61801, United States

S Supporting Information

ABSTRACT: Time release of encapsulated vinylene carbonate (VC) from microcapsules in Li-ion batteries is demonstrated to enhance the rate performance without sacrificing capacity retention. VC-filled microcapsules are successfully prepared by the solvent exchange method that allows VC to diffuse through the microcapsule shell wall at an elevated temperature. The concentration of VC added directly to the electrolyte in a pouch cell (2 wt %) significantly decreases after the first cycle at C/10-rate. In pouch cells that contain 5 wt % VC-filled microcapsules, the concentration of VC increases from 0 to 3 wt % over the first cycle because of the diffusion of microencapsulated VC in the electrolyte. Electrochemical impedance spectroscopy, rate capability, and long-term cycling tests are conducted for pouch cells with VC additives (0, 2, and 5 wt %) and VC microcapsules (5 wt %). Pouch cells with both 5 wt % VC additive and microencapsulated VC show improved capacity retention over 400 cycles at 1 C-rate compared to the cells without VC additive. When VC is added directly, the high initial concentration leads to increased interfacial resistance and decreased rate capability. By contrast, time release of microencapsulated VC by diffusion through microcapsules increases the discharge capacity 2.5 times at 5 C-rate compared to the direct VC addition to the electrolyte.

KEYWORDS: vinylene carbonate, battery additives, time release, microcapsules, lithium-ion batteries
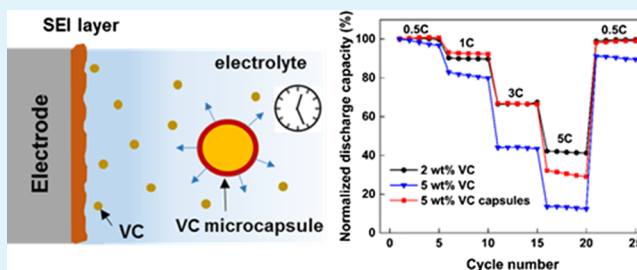
INTRODUCTION

In Li-ion batteries, electrolyte additives promote the formation of a stable solid-electrolyte interphase (SEI) layer at the interface between electrodes and electrolyte and increase long-term battery performance.[1,2] Without additives, the electrolyte decomposes on the electrode surface and forms unstable SEI layers.[3] The SEI layer builds up with continued cycling, reducing capacity retention by consuming lithium ions, contributing to the irreversible capacity, and increasing the cell resistance.[4,5] By contrast, additives react and form more stable SEI layers on electrodes prior to decomposition of the electrolyte.[2,6] One of the most common electrolyte additives is vinylene carbonate (VC). VC can be electrochemically reduced or oxidized on both electrodes to form stable SEI layers consisting of polymeric organic compounds and lithium salts (Figure S1 in the Supporting Information).[7,8] The addition of VC to the electrolyte enhances the capacity retention for Li-ion batteries with graphite- and silicon-based electrodes.[9–13]

Although VC additives extend the lifespan of batteries, the high concentration of VC during initial cycles increases cell interfacial resistance and diminishes the rate capability. Burns et al.[14,15] reported a trade-off between the capacity retention and the cell interfacial resistance when VC was added to the electrolyte. Initially, the capacity retention improved, but the cell interfacial resistance also increased because of the reaction of excess VC. High interfacial resistance in batteries

significantly diminishes the battery performance, especially at fast charge and discharge rates. For this reason, the initial VC concentration in the electrolyte is typically around 2 wt % to avoid increased cell resistance. The limited amount of VC is rapidly consumed during the initial charge and discharge cycles.[16] Once the VC additives are consumed, degradation in battery performance is accelerated with prolonged cycling.

Microencapsulation is an effective strategy for sequestering reactive core materials from the environment and provides an alternative approach to the incorporation of additives in batteries. Microcapsules have been extensively used to store and deliver chemical payloads for applications in the cosmetic, pharmaceutical, and agricultural industries.[17–19] Microcapsules containing polymerizing agents are also of interest for self-healing materials.[20–24] Delivery of encapsulated materials is controlled by the capsule size, shell wall materials and thickness, and the environment.

Microcapsules have recently been utilized in Li-ion batteries. Thermally triggered microspheres have enabled autonomous shutdown to prevent thermal runaway of batteries.[25] Baginska et al.[26] successfully encapsulated the additive 3-hexylthiophene which is electropolymerizable at high voltage and demonstrated

ex situ electropolymerization on a cathode. Kang et al.[27] reported the ex situ electrical restoration of nanoparticle Si electrodes using microencapsulated carbon black suspensions. Flame retardants were encapsulated in polymeric shell walls that melt at high temperature, releasing the additives only when needed.[28] However, microcapsules have not been used for the delivery of battery additives that promote a stable SEI layer formation.

In this study, we report a microcapsule-based strategy (Figure 1) to autonomously release VC additives during battery
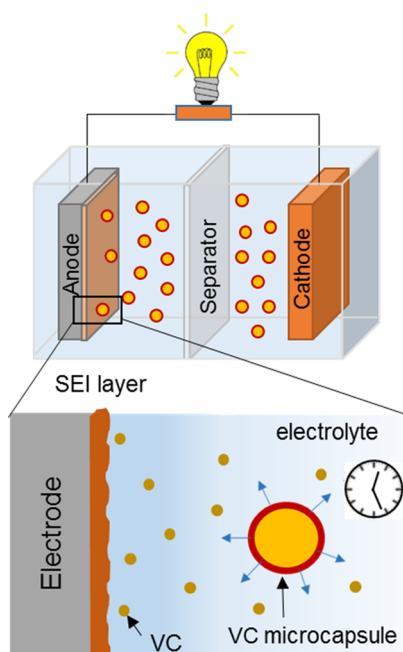

Figure 1. Schematic of microcapsule-based release of VC additives in a Li-ion battery.

operation. VC diffuses through the capsule shell wall during the initial stages of the SEI formation, minimizing any potential increase of the cell interfacial resistance. The capsules then continued to release VC after the first cycles to further reduce aging and degradation. We characterize the concentration of VC released from capsules in pure electrolyte as well as during electrochemical cycling of pouch cells. The cycling performance is compared to the pouch cells in which VC is directly added to the electrolyte.

■ EXPERIMENTAL SECTION

Materials. o-Dichlorobenzene (DCB), urea, formalin solution (37 w/v %), ammonium chloride, resorcinol, and hexyl acetate (HA) were purchased from Sigma-Aldrich. The polyurethane (PU) prepolymer, Desmodur L75, was provided by Bayer Materials Science and used as received. Ethylene-co-maleic anhydride (EMA) copolymer (Zemac-400) powder ($M_w \approx 400$ kDa) was obtained from Vertellus and used as a 2.5 wt % aqueous solution. VC and 1.2 M LiPF$_6$/EC:EMC (3/7 by weight) electrolyte were purchased from BASF. An Li-(Ni$_{0.8}$Co$_{0.15}$Al$_{0.05}$)O$_2$ (NCA) cathode (Quallion), a graphite (MAG-10) anode (Quallion), an Li(Ni$_{1/3}$Co$_{1/3}$Mn$_{1/3}$)O$_2$ (Li333) cathode (Enerland), and a mesocarbon microbead (MCMB) graphite anode (Enerland) were obtained from Argonne National Laboratory for electrochemical testing. Hardware components for the C2032-type coin cell, a separator (Celgard), and conductive nickel and aluminum tabs with an adhesive tape were purchased from MTI Corporation. An aluminum bag with polymer laminates was purchased from 3M Corporation.

Preparation of VC Microcapsules. VC microcapsules were prepared by the solvent exchange technique in which DCB-filled poly(urethane)/poly(urea-formaldehyde) (PU/PUF) double shell-walled microcapsules were immersed in VC liquid at an elevated temperature (Figure 2). The DCB-filled PU/PUF double shell-walled
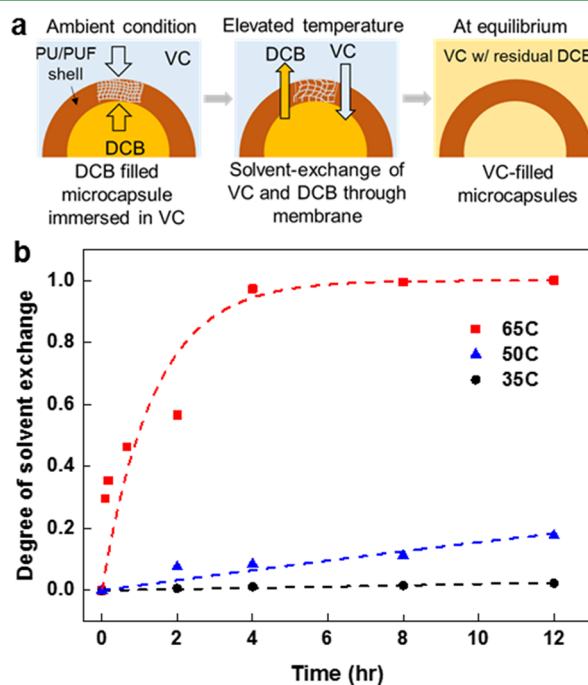

Figure 2. Preparation of VC-filled PU/PUF double shell-walled microcapsules using the solvent exchange method. (a) Schematic diagram of the solvent exchange process. (b) Temperature dependence of the solvent exchange process.

microcapsules were prepared by modifying an established encapsulation procedure.[27,29] Urea (1.8 g), ammonium chloride (0.18 g), and resorcinol (0.18 g) were dissolved to 120 mL of 1.25 wt % EMA aqueous solution. DCB (10 mL) that contained the PU prepolymer (0.13 g/mL) was added into the aqueous solution, emulsified for 5 min using a homogenizer (Omni GHL), and then mechanically stirred at 850 rpm. After formalin (4.8 g) was added, the emulsion was heated to 55 °C and maintained for 4 h. Microcapsules were separated by centrifugation and rinsed with deionized water, followed by freeze-drying. To prepare VC microcapsules, DCB-filled PU/PUF microcapsules (1 g) were added to VC liquid (5 g) and stored at 65 °C for a desired amount of time for solvent exchange. After the solution was cooled down, it was filtered without washing and air-dried to obtain VC-filled microcapsules. The solvent exchange process was performed in an Ar-filled glovebox to minimize water contamination of VC microcapsules, which is known to affect the battery performance.[30]

The degree of solvent exchange was quantified by measuring the ratio of DCB concentration in liquid media to theoretical equilibrium DCB concentration. Aliquots (0.2 mL) from the solvent exchange solution were taken at fixed time intervals and then syringe-filtered to remove the microcapsules. The filtrates were then analyzed by ^{1}H NMR. DCB concentration was calculated by comparing the characteristic peak integrals of DCB and VC.

Microcapsule Characterization. Microcapsule morphology was investigated by a scanning electron microscope (ESEM-FEG) and an optical microscope (Leica DMR). The size distributions of the microcapsules were determined by analyzing the scanning electron microscopy (SEM) images with ImageJ software. Thermogravimetric analysis (TGA) for microcapsules was performed on a Mettler-Toledo TGA851 instrument at a heating rate of 10 °C/min from 25 to 650 °C under an N$_2$ purge.
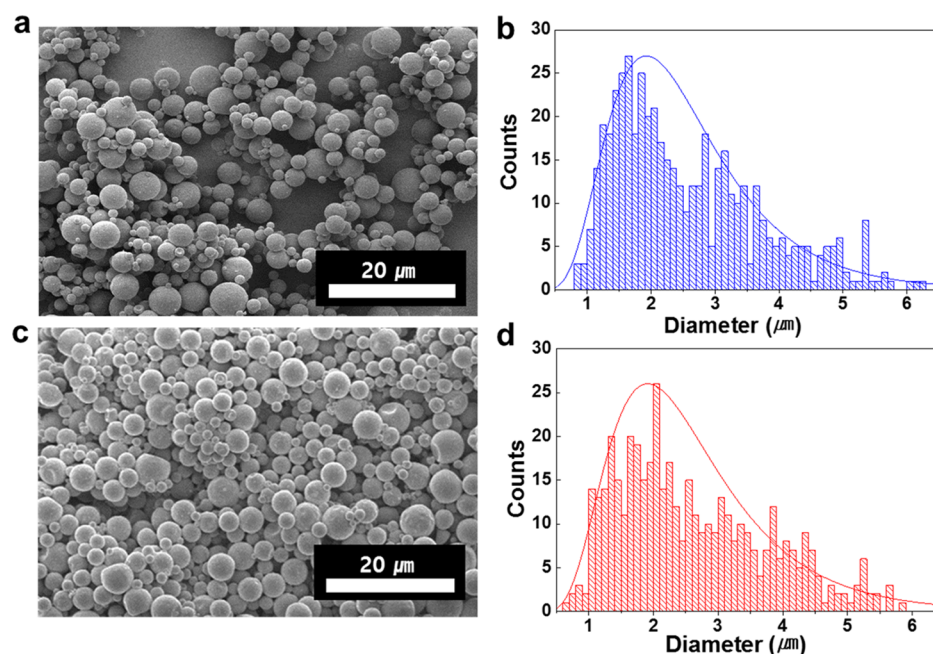
Figure 3. Microcapsule morphology and size distribution before and after the solvent exchange process: (a) SEM micrograph and (b) diameter histogram of DCB-filled microcapsules with an average diameter of 2.58 μm (before exchange) and (c) SEM micrograph and (d) diameter histogram of VC-filled microcapsules with an average diameter of 2.60 μm (after exchange).

Time-Release Profile of VC Microcapsules in the Battery Electrolyte. Release behavior of VC microcapsules in the battery electrolyte, 1.2 M LiPF$_6$/EC:EMC (3/7 by weight), was evaluated by nuclear magnetic resonance (^{1}H NMR, 500 MHz Varian VXR) experiments. VC microcapsules (0.556 g, 5 wt % VC) were added to the electrolyte (10 g) containing 1 wt % HA as an internal standard in the glovebox at room temperature. Aliquots (0.2 mL) of the electrolyte solution with microcapsules were taken at fixed time intervals and filtered for NMR analysis. Sample solutions were prepared with CDCl$_3$, and the VC concentration was calculated from the ratio of the characteristic peak integrals of VC and HA internal standard.

Battery Cell Assembly. The coin cells and aluminum pouch cells were assembled in an Ar-filled glovebox. The coin cells were prepared by using a commercial electric crimper (MTI Corporation). We also prepared coin cells with NCA and graphite (MAG-10) electrodes, a separator, and an electrolyte containing 5 wt % DCB to evaluate the effect of DCB on battery performance. For aluminum pouch cells, aluminum and nickel tabs with an adhesive polymer tape were spot-welded on the cathode and anode sides, respectively. Anode, separator, and cathode were stacked, rolled, and inserted into the aluminum pouch. After the electrolyte was added, the aluminum pouch was sealed using a vacuum heat sealer (SINBO DZ-280). For the time-release profiles of encapsulated VC and temperature change upon pouch cell cycling, we were unable to obtain the necessary quantity of MAG-10/NCA electrodes to fabricate the pouch cells with large electrodes. We substituted MCMB/Li333 electrodes for the time-release measurements, but for all other pouch cell tests, MAG-10/NCA electrodes were used to evaluate the battery performance.

Time-Release Profile of VC Microcapsules in Pouch Cells. VC concentrations in the electrolyte upon pouch cell cycling were measured by ^{1}H NMR (500 MHz Varian VXR). Aluminum pouch cells (MCMB/Li333, 140 mA h) were prepared in an Ar-filled glovebox with a 1.2 M LiPF$_6$/EC:EMC electrolyte (1.12 g) containing VC additive or VC-filled microcapsules. The amount of electrolyte used for the pouch cells was 8 mg/mA h, which is higher than the amount typically used in other studies ($\sim$3 mg/mA h).[14,16] After assembly, the pouch cells were taken out of the glovebox and mounted to the battery cycler (Arbin BT2000). Cells were cycled from 3.0 to 4.2 V at C/10-rate and disassembled to remove the electrolyte after each cycle in the Ar-filled glovebox. The electrolyte was extracted from

electrodes and separator by centrifugation, and 0.2 g of extracted electrolyte was mixed with 0.2 g of reference electrolyte (with 1 wt % HA, an internal standard). Sample solutions were prepared with CDCl$_3$, and the VC concentration was determined by comparing the characteristic peak integrals of VC and HA peaks.

Electrochemical Characterization. The pouch cells (MAG-10 graphite/NCA, 3 cm^2) with the electrolyte (0.4 g) including VC additive or VC microcapsules were cycled from 3.0 to 4.2 V at 1 C-rate after five formation cycles at C/10-rate. Electrochemical impedance spectroscopy (EIS) was conducted after the formation cycles at C/10-rate and then 100, 200, and 400 cycles at 1 C-rate over the frequency range of 5 mHz to 200 kHz at 3.72 V which is 50% of state-of-charge (SOC) using a Biologic VSP instrument.

The temperature change of the pouch cell during cycling was monitored using an infrared (IR) camera (FLIR SC620). To minimize refraction and improve accuracy of the IR measurement, we coated the surface of the pouch cell with black paint. The pouch cell (MCMB/Li333, 140 mA h) was cycled at C/10-rate at ambient conditions during temperature measurement.

RESULTS AND DISCUSSION

Encapsulation of VC. Microencapsulation of VC is challenging because VC is miscible with water as well as with most organic solvents except for highly nonpolar solvents such as hexane. Thus, oil-in-water (O/W) emulsion-based encapsulation techniques such as in situ polymerization[31] and solvent evaporation[32] are precluded. We first tried an oil-in-oil (O/O) emulsion using hydrocarbon solvents, but the resulting microcapsules were of poor quality with a low loading of VC in the core. To prepare microcapsules filled with high loading of VC in the core, we designed a microencapsulation method based on the solvent exchange technique that allows VC to diffuse into the core of as-prepared microcapsules at an elevated temperature. As a first step, we prepared o-dichlorobenzene (DCB)-filled PU/PUF double shell-walled microcapsules following the methods established by Caruso et al.[29] The DCB-filled microcapsules (1 g) were immersed in pure VC (5 g) for solvent exchange (Figure 2a). At ambient condition (T =

25 °C), diffusion of DCB and VC through the highly cross-linked PU/PUF shell wall membrane of the microcapsules is retarded, even though DCB and VC are highly miscible. At an elevated temperature (T = 65 °C), however, the shell wall membranes become more permeable to DCB and VC, resulting in an exchange of VC and DCB by diffusion.

We examined the temperature dependence of the solvent exchange of DCB with VC at 35, 50, and 65 °C (Figure 2b). The degree of solvent exchange was accessed by calculating the ratio of DCB concentration measured in liquid media to the theoretical equilibrium DCB concentration at time (t)

$$\text{Degree of solvent exchange} = \frac{C_{\text{DCB}}(t)}{C_{\text{DCB}}^{\text{Equil}}} \tag{1}$$

The time-dependent DCB concentration ($C_{\text{DCB}}(t)$) was determined by taking aliquots from the batch, filtering the microcapsules, and analyzing the filtrate with ^{1}H NMR. With solvent exchange, a DCB peak appeared in ^{1}H NMR of the filtrate and the peak intensity increased with time (Figure S2 in the Supporting Information). Little solvent exchange was observed at 35 °C. The solvent exchange ratio increased to 20% at 50 °C. At 65 °C, equilibrium and full exchange were reached within 12 h.

When microcapsules are placed in organic solvents, the cross-linked shell wall membrane swells and the mesh size of the crosslinking network increases.[33] If the membrane is not swelled enough and the mesh size is too small compared to the molecular size of the solvent, molecules do not penetrate the membrane.[34] Higher temperatures favor solvent absorption, and the mesh size of the crosslinking network increases enough for DCB and VC to exchange through the membrane by diffusion.

Characterization of VC Microcapsules. Figure 3 contains SEM images and size distribution histograms of the micro-capsules before and after the solvent exchange process. The microcapsule size distributions were obtained by SEM image analysis. The microcapsules in both cases were spherical with a smooth surface (Figure 3a,c). The average size of the microcapsules remained unchanged (2.6 ± 1.1 μm), as shown in Figure 3b,d, with no noticeable change in morphology during the solvent exchange process.

To analyze the amount of VC in microcapsules, we performed dynamic TGA of the DCB microcapsules, VC microcapsules, and authentic VC liquid (Figure 4). DCB has a boiling point of 180 °C, and the DCB-filled capsules remain stable to over 200 °C. By contrast, VC microcapsules showed mass losses starting at 50 °C and extending to 175 °C. The relative content of the VC microcapsules core was calculated from peak integrals of the mass loss rate as 96 wt % VC and 4 wt % DCB (Figure 4b).

Time Release of VC in the Electrolyte. Time release of VC additives from microcapsules in the battery electrolyte, 1.2 M LiPF$_6$/EC:EMC (3:7 by weight), was evaluated at room temperature. The release percentage of VC microcapsules during 8 days is shown in Figure 5a. The VC microcapsules released ~65% of the VC core liquid in the first 4 h and nearly 75% of the initial core material after 8 days. In longer-term testing (Figure 5b), VC microcapsules continued to release VC slowly, and the release percentage from VC capsules after 35 days was 96%.

Ideally, the release behavior of microcapsules in liquid media is described by Fick's diffusion, unless the shell wall material
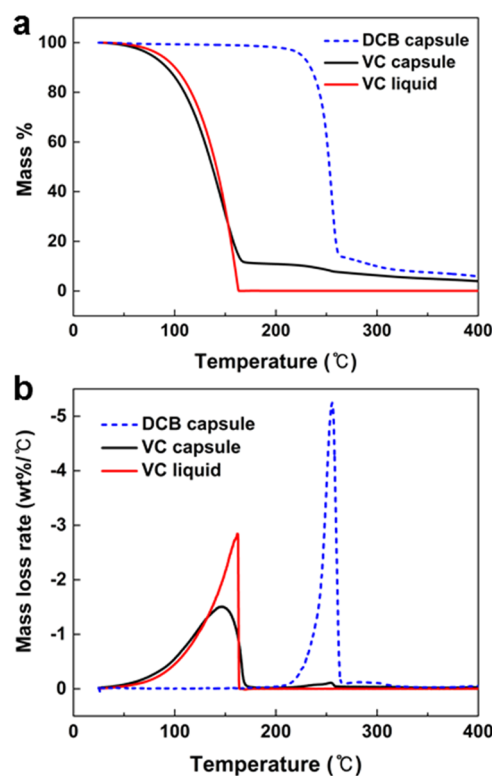
Figure 4. Microcapsule content and thermal stability for DCB-filled microcapsules, VC-filled microcapsules, and authentic VC liquid. (a) TGA weight loss curves and (b) derivatives of TGA curves.
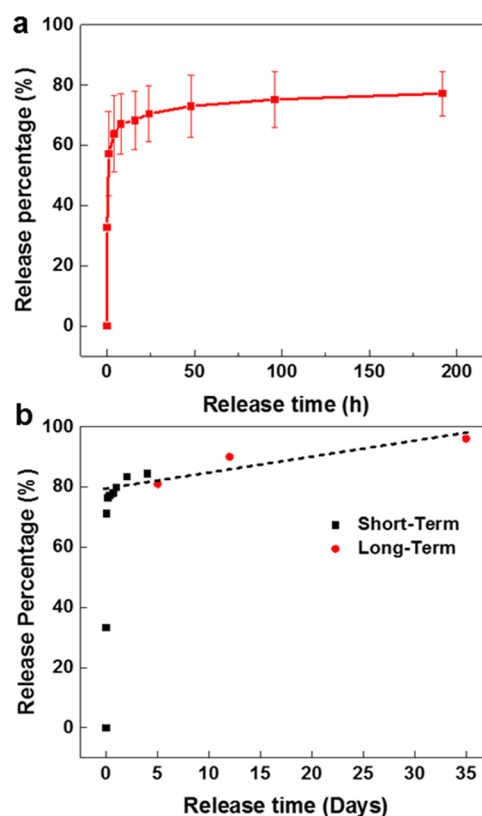

Figure 5. Release profile of VC microcapsules in battery electrolyte, (a) over 8 days (192 h) and (b) over long-term 35 days.

degrades.[35,36] The release rate increases as the capsule size and shell wall thickness decrease. The VC microcapsules have an average diameter of 2.6 ± 1.1 μm, and the specific surface area was 12 800 cm^2/g. A shell wall thickness of 120 nm was measured from the SEM images of sectioned microcapsules embedded in the epoxy matrix (Figure S3 in the Supporting Information). The immersion liquid also affects the release rate of microcapsules. Sun et al.[37] reported that the release rate of core liquid of double-layered polyurea microcapsules increased with the polarity of the immersion solvent. Higher solvent polarity increases swelling and the release rate of core materials. The initial release rate of VC capsules in the electrolyte was faster than that of DCB capsules in pure VC liquid at solvent exchange. We hypothesize that the initial rapid release of VC microcapsules in the electrolyte is due to the higher polarity of the electrolyte (1.2 M LiPF$_6$ in EC/DMC) compared to pure VC. In addition, VC is more compatible with EC/DMC than DCB.

Time Release of VC during Battery Cycling. The initial rapid release behavior of VC microcapsules in the electrolyte is beneficial for battery performance. When battery cells are first charged, cell voltage increases from the open-circuit voltage and an SEI layer forms by electrochemical reaction of VC additives at the electrode–electrolyte interface within a few minutes.[7] VC microcapsules have the potential to release a desirable amount of VC (2−3 wt %) that is required to form the SEI layer at the initial stage and then slowly release additional amounts of VC to stabilize the electrode–electrolyte interface over prolonged cycles.

Figure 6 shows the resulting VC concentration profiles upon battery cycling. In pouch cells where 2 wt % VC additive was
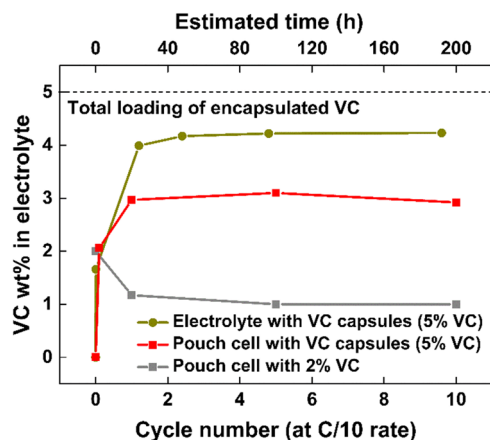
Figure 6. VC concentration profile in the electrolyte as a function of cycle number for pouch cells (MCMB/Li333) with VC additives (2 wt %) and VC microcapsules (5 wt %). The VC concentration profile for the electrolyte with VC microcapsules (5 wt %) without pouch cell cycling was based on time (upper x-axis).

mixed directly in the electrolyte, the VC concentration decreased to 1 wt % after the first cycle and did not change after 10 cycles. The VC concentration of 1 wt % is too low to form the stable SEI for continued cycling. By contrast, for pouch cells that contained VC microcapsules (5 wt % VC), the VC concentration increased from 2 to 3 wt % during the first cycle and was maintained at ∼3 wt % for the next 9 cycles. Hence, the pouch cells with VC microcapsules were cycled at nearly constant VC concentration that is sufficient to form a

stable SEI layer and much lower than the initial VC loading of 5 wt %.

For comparison, the release curve for VC microcapsules immersed in the electrolyte (5 wt % VC) without battery cycling is also plotted in Figure 6. For pouch cells with VC microcapsules, VC concentrations after the first cycle were about 1 wt % lower than those for VC microcapsules immersed in the electrolyte without cycling. We attribute this concentration difference to VC consumption for the SEI layer formation during the first cycle. In pouch cells where 2 wt % VC was added directly to the electrolyte (no capsule), the VC concentration profile decreased to 1 wt % after the first cycle. The amount of VC additives consumed for the SEI layer formation during the first cycle was calculated as 80 μg/mA h at C/10-rate and was nearly the same for the pouch cells with encapsulated VC (5 wt % VC) and directly added VC (2 wt %).

The temperature of pouch cells during the first cycle at C/10-rate was measured with an infrared camera. As shown in Figure S4 (in the Supporting Information), the average temperature during cycle was 23.2 ± 0.2 °C, and the temperature change was negligible. Thus, there was no significant temperature effect on the release behavior of encapsulated VC during our cycling experiments.

Effect of VC Time Release on Electrochemical Performance. To evaluate the electrochemical performance for our VC microcapsules battery system, we conducted EIS, cycling tests at various C-rates, as well as long-term cycling tests for pouch cells containing no VC (0 wt %), VC additives (2 and 5 wt %), and VC microcapsules (5 wt % VC). We first examined the effect of any residual DCB in the microcapsules on the battery performance. Coin cells were fabricated with pure electrolyte or electrolyte containing 5 wt % DCB. The cyclic voltammetry curves and cycling test results of both coin cells were identical (Figure S5 in the Supporting Information). Hence, small amounts of residual DCB are not expected to influence the electrochemical performance of the pouch cells.

Figure 7a shows the impedance results for the pouch cells with 0, 2, and 5 wt % VC directly added to the electrolyte, and the pouch cells with electrolyte containing VC microcapsules (5 wt % VC). The EIS measurements were conducted after the pouch cells had 5 formation cycles at C/10-rate. The cell interfacial resistance which is a combination of the SEI film resistance and charge-transfer resistance was determined from the resistive values extracted by fitting to the proposed equivalent circuit model (Figure 7a).[38,39] The cell interfacial resistance increased with increasing addition of VC directly added to the electrolyte. By contrast, the cell interfacial resistance for the pouch cell with VC microcapsules (5 wt % VC) was much smaller than the pouch cell with the same total amount of VC additive (not encapsulated), and only slightly larger than the pouch cell with 2 wt % VC directly added to the electrolyte. During the first cycle, the VC concentration of the pouch cell with VC microcapsules ranged from 2 to 3 wt % (Figure 6) and was slightly higher than the concentration of 2 wt % VC added directly. Hence, the time release of VC from microcapsules provides a mechanism to increase the total amount of VC available to the battery without significantly increasing the cell interfacial resistance.
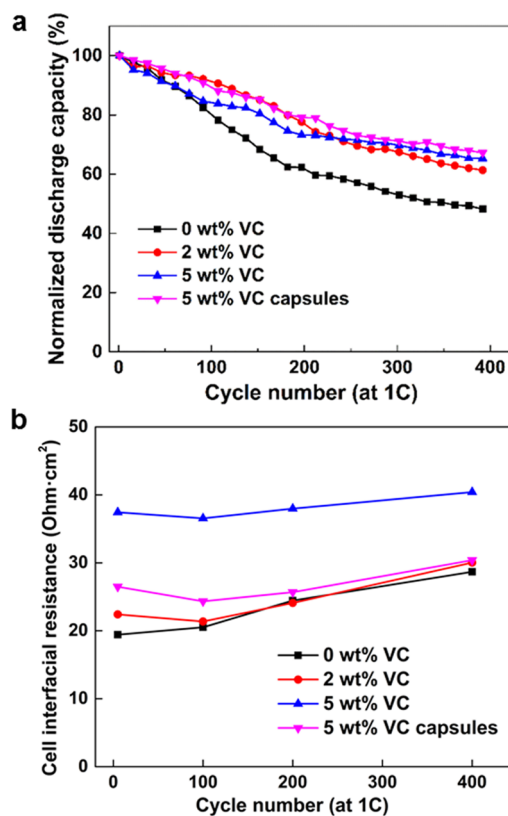
Discharge capacity at different cycling rates was also studied for the pouch cells with VC microcapsules and VC additives added directly. As shown in Figure 7b, the pouch cell with VC microcapsules showed better capacity retention than the pouch cell with the same amount of VC added directly to the
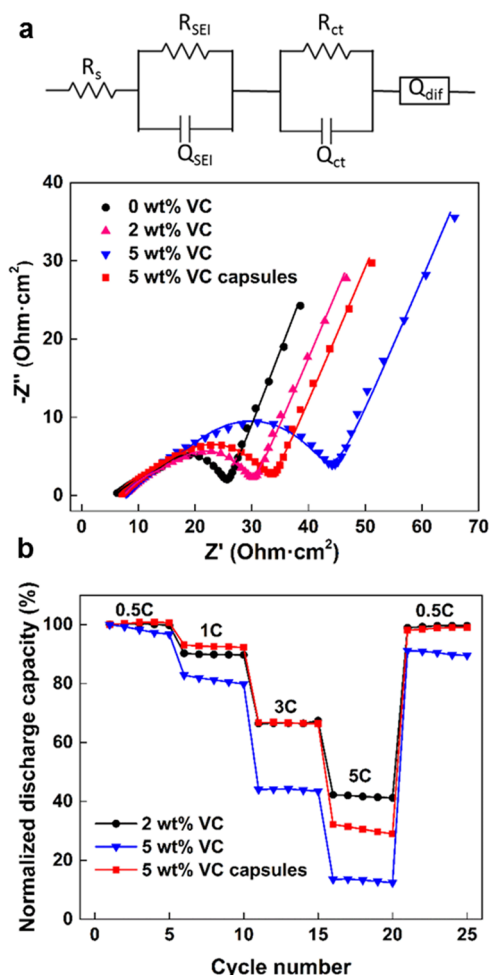
Figure 7. Electrochemical performance of pouch cells (MAG-10/NCA) with electrolyte including VC additives or VC microcapsules. (a) Simulated circuit diagram and impedance spectra (symbols) with fitting results (lines) after five cycles at C/10-rate, and (b) capacity retention at various C-rates.

Figure 8. Long-term capacity retention (a) and cell interfacial resistance (b) for the pouch cells (MAG-10/NCA) containing VC additives (0, 2, and 5 wt %) and VC microcapsules (5 wt %) in the electrolyte over 400 cycles at 1 C-rate.

electrolyte. The rate capability became more pronounced at higher charging and discharging rates, and at 5 C-rate, normalized discharge capacity of the pouch cell with VC microcapsules was 2.5 times higher than that of the pouch cell where the same amount of VC was added directly (5 wt % VC). Compared to the pouch cell with 2 wt % VC added directly, the pouch cell with VC microcapsules showed similar capacity retention up to 3 C-rate except for at 5 C-rate. We attribute the improved rate capability of pouch cells with VC microcapsules to lower cell interfacial resistance.

The long-term cycling performance of the pouch cells was also evaluated (Figure 8). The pouch cells were charged and discharged up to 400 cycles at 1 C-rate at room temperature. For the pouch cell with no VC, the discharge capacity decreased down to 50% of its initial capacity after 400 cycles. However, for the pouch cell where 2 and 5 wt % VC was added directly into the electrolyte, the capacity retention was improved because of the beneficial interfacial reaction of VC additives for more stable SEI formation. The pouch cell with VC microcapsules showed similar capacity retention as the pouch cell with 5 wt % VC (not encapsulated). We also monitored the changes of cell interfacial resistance for the pouch cells with electrolyte containing 0, 2, and 5 wt % VC

(not encapsulated) or 5 wt % encapsulated VC (Figure 8b). As expected, the cell interfacial resistance of the pouch cell with 2 wt % VC was only slightly higher resistance (30 $\Omega \cdot cm^2$) after 400 cycles than the pouch cell with 0 wt % VC (29 $\Omega \cdot cm^2$). In the pouch cell with 5 wt % encapsulated VC in the electrolyte, cell interfacial resistance after 400 cycles was the same as 2 wt % VC and was significantly lower than that of the pouch cell with 5 wt % VC additives (40 $\Omega \cdot cm^2$). To better elucidate the potential advantage of the cell with 5 wt % encapsulated VC relative to the cell with 2 wt % VC, we also plotted Figure 8b in terms of normalized cell interfacial resistance (Figure S6 in the Supporting Information). The rate of increase in resistance during 400 cycles is much smaller for the 5 wt % encapsulated VC than that of the 2 wt % VC. Hence, the release of microencapsulated VC provides a method to enhance the rate capability of lithium-ion batteries without sacrificing capacity retention.

■ CONCLUSIONS

An autonomous strategy to enhance the rate capability of lithium-ion batteries without sacrificing capacity retention was demonstrated using the time release of microencapsulated VC additives. VC-filled microcapsules (2.6 μm) were successfully prepared by a solvent exchange encapsulation method, which allowed VC to diffuse into microcapsules at an elevated temperature (65 °C). In pouch cells with VC microcapsules (5 wt % VC), microcapsules released a sufficient amount (2−3 wt %) of VC to form stable SEI layers at the first cycle, and subsequent slow release of VC maintained VC concentration at 3 wt %. The interfacial resistance for pouch cells with VC

microcapsules (5 wt %) was much lower than that of pouch cells with the same amount of VC additive (not encapsulated), which also led to the improved rate capabilities. During 400 cycles at 1 C-rate, the pouch cell with VC microcapsules (5 wt % VC) showed similar capacity retention compared to pouch cell with 5 wt % VC (not encapsulated). The microcapsule-based time-release approach demonstrated for VC is general and has potential for delivery of other active materials and additives to enhance the performance in lithium-ion batteries.

■ ASSOCIATED CONTENT

Ⓢ Supporting Information

The Supporting Information is available free of charge on the ACS Publications website at DOI: 10.1021/acsami.7b12169.

Proposed electrochemical reduction mechanism of VC in SEI formation, ^{1}H NMR spectra for the filtrates during solvent exchange, SEM image of sectioned microcapsules embedded in epoxy matrix, temperature measurement using IR camera for the pouch cell (MCMB/Li333), electrochemical characterization for coin cells with electrolyte containing 0 and 5 wt % DCB, and normalized interfacial cell resistance of the pouch cells during 400 cycles (PDF)

■ AUTHOR INFORMATION

Corresponding Author

*E-mail: n-sottos@illinois.edu.

ORCID Ⓘ

Nancy R. Sottos: 0000-0002-5818-520X

Present Address

∥Decontamination & Decommissioning Research Division, Korea Atomic Energy Research Institute, 111 Daedeok-daero, 989 Beon-gil, Yuseong-gu, Daejeon, South Korea (C.W. Park).

Notes

The authors declare no competing financial interest.

■ ACKNOWLEDGMENTS

■ REFERENCES

(1) Zhang, S. S. A Review on Electrolyte Additives for Lithium-Ion Batteries. *J. Power Sources* **2006**, *162*, 1379−1394.

(2) Xia, J.; Ma, L.; Dahn, J. R. Improving the Long-Term Cycling Performance of Lithium-Ion Batteries at Elevated Temperature with Electrolyte Additives. *J. Power Sources* **2015**, *287*, 377−385.

(3) Lawder, M. T.; Northrop, P. W. C.; Subramanian, V. R. Model-Based SEI Layer Growth and Capacity Fade Analysis for EV and PHEV Batteries and Drive Cycles. *J. Electrochem. Soc.* **2014**, *161*, A2099−A2108.

(4) Ramadass, P.; Haran, B.; White, R.; Popov, B. N. Capacity Fade of Sony 18650 Cells Cycled at Elevated Temperatures: Part I. Cycling Performance. *J. Power Sources* **2002**, *112*, 606−613.

(5) Ploehn, H. J.; Ramadass, P.; White, R. E. Solvent Diffusion Model for Aging of Lithium-Ion Battery Cells. *J. Electrochem. Soc.* **2004**, *151*, A456−A462.

(6) Zhao, X.; Zhuang, Q.-C.; Shi, Y.-L.; Zhang, X.-X. Influence of Vinylene Carbonate as an Additive on the Electrochemical Performances of Graphite Electrode in Poly(Methyl Methacrylate) Gel Polymer Electrolytes. *J. Appl. Electrochem.* **2015**, *45*, 1013−1023.

(7) El Ouatani, L.; Dedryvère, R.; Siret, C.; Biensan, P.; Reynaud, S.; Iratçabal, P.; Gonbeau, D. The Effect of Vinylene Carbonate Additive on Surface Film Formation on Both Electrodes in Li-Ion Batteries. *J. Electrochem. Soc.* **2009**, *156*, A103−A113.

(8) El Ouatani, L.; Dedryvère, R.; Siret, C.; Biensan, P.; Gonbeau, D. Effect of Vinylene Carbonate Additive in Li-Ion Batteries: Comparison of LiCoO2/C, LiFePO4/C, and LiCoO2/Li4Ti5O12 Systems. *J. Electrochem. Soc.* **2009**, *156*, A468−A477.

(9) Burns, J. C.; Sinha, N. N.; Coyle, D. J.; Jain, G.; VanElzen, C. M.; Lamanna, W. M.; Xiao, A.; Scott, E.; Gardner, J. P.; Dahn, J. R. The Impact of Varying the Concentration of Vinylene Carbonate Electrolyte Additive in Wound Li-Ion Cells. *J. Electrochem. Soc.* **2012**, *159*, A85−A90.

(10) Chen, L.; Wang, K.; Xie, X.; Xie, J. Enhancing Electrochemical Performance of Silicon Film Anode by Vinylene Carbonate Electrolyte Additive. *Electrochem. Solid-State Lett.* **2006**, *9*, A512−A515.

(11) Chen, L.; Wang, K.; Xie, X.; Xie, J. Effect of Vinylene Carbonate (VC) as Electrolyte Additive on Electrochemical Performance of Si Film Anode for Lithium Ion Batteries. *J. Power Sources* **2007**, *174*, 538−543.

(12) Krueger, S.; Kloepsch, R.; Li, J.; Nowak, S.; Passerini, S.; Winter, M. How Do Reactions at the Anode/Electrolyte Interface Determine the Cathode Performance in Lithium-Ion Batteries? *J. Electrochem. Soc.* **2013**, *160*, A542−A548.

(13) Profatilova, I. A.; Stock, C.; Schmitz, A.; Passerini, S.; Winter, M. Enhanced Thermal Stability of a Lithiated Nano-Silicon Electrode by Fluoroethylene Carbonate and Vinylene Carbonate. *J. Power Sources* **2013**, *222*, 140−149.

(14) Burns, J. C.; Petibon, R.; Nelson, K. J.; Sinha, N. N.; Kassam, A.; Way, B. M.; Dahn, J. R. Studies of the Effect of Varying Vinylene Carbonate (VC) Content in Lithium Ion Cells on Cycling Performance and Cell Impedance. *J. Electrochem. Soc.* **2013**, *160*, A1668−A1674.

(15) Petibon, R.; Henry, E. C.; Burns, J. C.; Sinha, N. N.; Dahn, J. R. Comparative Study of Vinyl Ethylene Carbonate (VEC) and Vinylene Carbonate (VC) in LiCoO2/Graphite Pouch Cells Using High Precision Coulometry and Electrochemical Impedance Spectroscopy Measurements on Symmetric Cells. *J. Electrochem. Soc.* **2014**, *161*, A66−A74.

(16) Petibon, R.; Xia, J.; Burns, J. C.; Dahn, J. R. Study of the Consumption of Vinylene Carbonate in Li[Ni0.33Mn0.33Co0.33]O2/ Graphite Pouch Cells. *J. Electrochem. Soc.* **2014**, *161*, A1618−A1624.

(17) Kakran, M.; Antipina, M. N. Emulsion-Based Techniques for Encapsulation in Biomedicine, Food And Personal Care. *Curr. Opin. Pharmacol.* **2014**, *18*, 47−55.

(18) Lee, H.; Choi, C.-H.; Abbaspourrad, A.; Wesner, C.; Caggioni, M.; Zhu, T.; Weitz, D. A. Encapsulation and Enhanced Retention of Fragrance in Polymer Microcapsules. *ACS Appl. Mater. Interfaces* **2016**, *8*, 4007−4013.

(19) Yuan, H.; Li, G.; Yang, L.; Yan, X.; Yang, D. Development of Melamine−Formaldehyde Resin Microcapsules with Low Formaldehyde Emission Suited for Seed Treatment. *Colloids Surf., B* **2015**, *128*, 149−154.

(20) Celestine, A.-D. N.; Sottos, N. R.; White, S. R. Autonomic Healing of PMMA via Microencapsulated Solvent. *Polymer* **2015**, *69*, 241−248.

(21) Cho, S. H.; White, S. R.; Braun, P. V. Room-Temperature Polydimethylsiloxane-Based Self-Healing Polymers. *Chem. Mater.* **2012**, *24*, 4209−4214.

(22) Diesendruck, C. E.; Sottos, N. R.; Moore, J. S.; White, S. R. Biomimetic Self-Healing. *Angew. Chem., Int. Ed.* **2015**, *54*, 10428−10447.

(23) Jin, H.; Mangun, C. L.; Griffin, A. S.; Moore, J. S.; Sottos, N. R.; White, S. R. Thermally Stable Autonomic Healing in Epoxy Using a Dual-Microcapsule System. *Adv. Mater.* **2014**, *26*, 282−287.

(24) White, S. R.; Sottos, N. R.; Geubelle, P. H.; Moore, J. S.; Kessler, M. R.; Sriram, S. R.; Brown, E. N.; Viswanathan, S. Autonomic Healing of Polymer Composites. *Nature* **2001**, *409*, 794−797.

(25) Baginska, M.; Blaiszik, B. J.; Merriman, R. J.; Sottos, N. R.; Moore, J. S.; White, S. R. Autonomic Shutdown of Lithium-Ion Batteries Using Thermoresponsive Microspheres. *Adv. Energy Mater.* **2012**, *2*, 583−590.

(26) Baginska, M.; Kaitz, J. A.; Jones, A. R.; Long, B. R.; Gewirth, A. A.; Sottos, N. R.; Moore, J. S.; White, S. R. Electropolymerization of Microencapsulated 3-hexylthiophene for Lithium-Ion Battery Applications. *J. Electrochem. Soc.* **2015**, *162*, A373−A377.

(27) Kang, S.; Jones, A. R.; Moore, J. S.; White, S. R.; Sottos, N. R. Microencapsulated Carbon Black Suspensions for Restoration of Electrical Conductivity. *Adv. Funct. Mater.* **2014**, *24*, 2947−2956.

(28) Yim, T.; Park, M.-S.; Woo, S.-G.; Kwon, H.-K.; Yoo, J.-K.; Jung, Y. S.; Kim, K. J.; Yu, J.-S.; Kim, Y.-J. Self-Extinguishing Lithium Ion Batteries Based on Internally Embedded Fire-Extinguishing Microcapsules with Temperature-Responsiveness. *Nano Lett.* **2015**, *15*, 5059−5067.

(29) Caruso, M. M.; Blaiszik, B. J.; Jin, H.; Schelkopf, S. R.; Stradley, D. S.; Sottos, N. R.; White, S. R.; Moore, J. S. Robust, Double-Walled Microcapsules for Self-Healing Polymeric Materials. *ACS Appl. Mater. Interfaces* **2010**, *2*, 1195−1199.

(30) Zheng, L.-Q.; Li, S.-J.; Lin, H.-J.; Miao, Y.-Y.; Zhu, L.; Zhang, Z.-J. Effects of Water Contamination on the Electrical Properties of 18650 Lithium-Ion Batteries. *Russ. J. Electrochem.* **2014**, *50*, 904−907.

(31) Brown, E. N.; Kessler, M. R.; Sottos, N. R.; White, S. R. In situ Poly(urea-formaldehyde) Microencapsulation of Dicyclopentadiene. *J. Microencapsulation* **2003**, *20*, 719−730.

(32) Shirin-Abadi, A. R.; Mahdavian, A. R.; Khoee, S. New Approach for the Elucidation of PCM Nanocapsules through Miniemulsion Polymerization with an Acrylic Shell. *Macromolecules* **2011**, *44*, 7405−7414.

(33) Canal, T.; Peppas, N. A. Correlation Between Mesh Size Aand Equilibrium Degree of Swelling of Polymeric Networks. *J. Biomed. Mater. Res.* **1989**, *23*, 1183−1193.

(34) Peppas, N. A.; Lustig, S. R. The Role of Cross-links, Entanglements, and Relaxations of the Macromolecular Carrier in the Diffusional Release of Biologically Active Materialsa. *Ann. N.Y. Acad. Sci.* **1985**, *446*, 26−40.

(35) Bachtsi, A. R.; Kiparissides, C. Synthesis and Release Studies of Oil-Containing Poly(Vinyl Alcohol) Microcapsules Prepared by Coacervation. *J. Controlled Release* **1996**, *38*, 49−58.

(36) Yuan, L.; Liang, G.-Z.; Xie, J.-Q.; Li, L.; Guo, J. The Permeability and Stability of Microencapsulated Epoxy Resins. *J. Mater. Sci.* **2007**, *42*, 4390−4397.

(37) Sun, D.; An, J.; Wu, G.; Yang, J. Double-Layered Reactive Microcapsules with Excellent Thermal and Non-Polar Solvent Resistance for Self-Healing Coatings. *J. Mater. Chem. A* **2015**, *3*, 4435−4444.

(38) Chen, C. H.; Liu, J.; Amine, K. Symmetric Cell Approach and Impedance Spectroscopy of High Power Lithium-Ion Batteries. *J. Power Sources* **2001**, *96*, 321−328.

(39) Waag, W.; Käbitz, S.; Sauer, D. U. Experimental Investigation of the Lithium-Ion Battery Impedance Characteristic at Various Conditions and Aging States and its Influence on the Application. *Appl. Energy* **2013**, *102*, 885−897.